

spectrometry could resolve the relative intensities in the branches of a decay scheme such as that of  $\text{Kr}^{79}-\text{Br}^{79}$ , if a field-free collection volume were used, as in the embodiment of our apparatus that was used in studying the momentum spectrum of the single-line neutrino recoils of  $\text{A}^{37}$ .<sup>5</sup> Separate momentum spectra would have

to be taken in several of the charge states, and the demand upon the supply of the radio-nuclide would be heavy. With a cyclotron-produced nuclide such as  $\text{Kr}^{79}$ , factors of gas economy would demand severe modifications in our present equipment in order to bring such an experiment, attractive as it is, within practical reach.

## Neutron Yields from Targets Bombarded by Electrons\*

W. C. BARBER AND W. D. GEORGE†

*High-Energy Physics Laboratory, Stanford University, Stanford, California*

(Received July 21, 1959)

The total neutron yields from thick targets bombarded by electrons were measured as a function of electron energy for the range 10 to 36 Mev. Targets ranging in thickness from one to six radiation lengths of C, Al, Cu, Ta, Pb, and U were used. The yields for 1- and 6-radiation-length targets of Pb at 34 Mev are  $2.1 \times 10^{-3}$  and  $9.0 \times 10^{-3}$  neutrons/electron. Extrapolation to infinite target thickness gives a value of  $9.5 \times 10^{-3}$  neutron/electron. The yield, comparing targets of one radiation length, from C is about 10 times smaller and that from U two times greater than the yield from Pb. An explanation of the relative  $Z$ -dependence of the yield in terms of known photonuclear cross sections is successful to within a factor of 1.5. The absolute accuracy of the results is estimated to be  $\pm 15\%$ .

Calibration of the neutron-detecting equipment was made with a RaBe source and checked by measuring the yields, due to electro- and photodisintegration of the deuteron, from a heavy-water target. In addition, yields from thin targets of Be and Cu were observed as a function of electron energy. The data for Be yield a value of  $(0.018 \pm 0.003)$  Mev-barn for the  $(\gamma, n)$  cross section integrated to 17 Mev. The data for Cu were analyzed and combined with other measurements to give an approximate cross section for the  $\text{Cu}(\gamma, pn)$  reaction.

### INTRODUCTION

THE yield of neutrons from targets bombarded by an electron beam is interesting from the viewpoint of understanding the nuclear processes involved in the production of neutrons, as well as for the practical reason that electron beams are becoming increasingly important as neutron sources. If the target is thick (about one radiation length or more), the incident electron beam generates a cascade shower of lesser-energy electrons and photons, and neutrons are produced primarily by the photons interacting with the nucleus in the "giant" resonance region. (The direct interaction of electrons with the nucleus is of the order of  $\alpha$  times weaker than the interaction of photons and is therefore of little importance.) The neutron yield from any target could be calculated if the photonuclear cross section were known and a valid shower theory were available. At the present time neither of these requirements is fulfilled to a satisfactory degree. In particular, the shower theory is incomplete at energies near or below the critical energy, and this includes the giant resonance for all except the heaviest nuclei. A calculation of neutron yields from a thick uranium

target has been made by Biram,<sup>1</sup> and measurements using uranium targets have been reported from Harwell<sup>2</sup> and by Baldwin *et al.*<sup>3</sup>

Our work extends the measurements to a variety of target materials and thicknesses. The Stanford Mark II accelerator<sup>4</sup> served as the source of electrons with energies variable from 10 to 36 Mev.<sup>5</sup> The results show a strong dependence of the yield on the atomic number of the target. In the discussion the observed  $Z$ -dependence is compared with the results predicted from measured cross sections and cascade shower theory. In spite of the fact that the shower theory is approximate, the agreement with experiment is satisfactory. Knowledge of this  $Z$ -dependence of the neutron yield can be used to minimize neutron production in shielding x-ray or electron beams. The neutron shielding requirements will depend on the energy spectrum as well as on the total number of neutrons produced. Measurements of the energy spectra of photoneutrons have been made recently,<sup>6-8</sup> and can be used in conjunction with the

<sup>1</sup> M. B. Biram, Atomic Energy Research Establishment, Harwell Report T/R 1523, 1954 (unpublished).

<sup>2</sup> E. Bretscher (private communication to G. A. Kolstad).

<sup>3</sup> Baldwin, Gaertner, and Yeater, *Phys. Rev.* **104**, 1652 (1956).

<sup>4</sup> R. F. Post and N. S. Shiren, *Rev. Sci. Instr.* **26**, 205 (1955).

<sup>5</sup> Increased to 45 Mev since these experiments were finished.

<sup>6</sup> Cortini, Milone, Rubbino, and Ferrero, *Nuovo cimento* **9**, 85 (1958).

<sup>7</sup> Cavallaro, Emma, Milone, and Rubbino, *Nuovo cimento* **9**, 736 (1958).

<sup>8</sup> Bertozzi, Paolini, and Sargent, *Phys. Rev.* **110**, 790 (1958).

\* Supported by the joint program of the Office of Naval Research, the U. S. Atomic Energy Commission, and the Air Force Office of Scientific Research.

† Now at Aerospace Division, Boeing Airplane Company, Seattle 24, Washington.

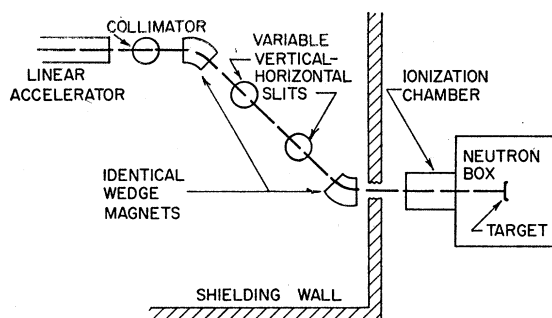


FIG. 1. Block diagram of experimental arrangement.

total yields presented here to calculate shielding requirements.

In addition to work with thick targets, some yield curves from thin targets were measured. In this case the interpretation of the results is complicated by the approximately equal contributions of the direct neutron production by electrons and production by photons. A separation of these effects was made using stacked-foil methods similar to those of Brown and Wilson<sup>9</sup> and of Barber.<sup>10</sup>

The neutron yield from the deuterons in a heavy-water target was measured to calibrate the neutron detectors. The total cross section as a function of photon energy is known to about 10% accuracy, and the efficiency of the detecting system, determined with a standard RaBe source, was checked to this extent.

Yield curves from thin Be and Cu targets were analyzed by the photon-difference method to obtain  $(\gamma, n)$  cross sections. In the discussion a comparison of results is presented, and a combination of these results with previous measurements is used to derive an approximate cross section for the previously unstudied  $\text{Cu}(\gamma, pn)$  reaction.

#### EXPERIMENTAL APPARATUS AND ARRANGEMENT

The configuration of the experimental equipment is shown in Fig. 1. The electron beam of energy  $E_0$  was obtained from the achromatic beam translation system of the Mark II linear accelerator. This system, comprised of twin 30° deflecting magnets, produced an external beam free of background radiation and particles. A circular collimator of 0.187-in diameter, placed in the system ahead of the deflection magnets, produced a beam spot at the target position approximately 0.5 in. in diameter at 30 Mev. An energy spread of  $\Delta E_0/E_0 = 2\%$  was used throughout the experiment. The energy of the electron beam was calibrated to within  $\pm 2\%$  error using the photoneutron thresholds of deuterium, oxygen, and copper. The beam was variable in energy up to a maximum of 36 Mev.

The electron intensity was monitored by a hydrogen-filled ionization chamber placed in the incident beam

directly ahead of the target. The chamber had a collecting field transverse to the beam so that the total material traversed by the beam before striking the target was 8 in. of hydrogen gas and 0.005 in. of Mylar window material. Hydrogen flowed continuously through the chamber at atmospheric pressure. The response of this chamber as a function of primary beam energy was studied previously.<sup>11</sup> For the present measurements it was recalibrated at a few energy points by the method employed previously, comparison with a Faraday-cup monitor.

The target was located in a Lucite vacuum chamber 8 in. in diameter and 19 in. long. A sliding vacuum seal permitted the choice of two target positions. Lucite was chosen as the most suitable material for the vacuum chamber because its constituents have low cross sections and high thresholds for  $(\gamma, n)$  reactions. All targets were  $4\frac{1}{2}$  in. square, so that even at very low electron energies multiple scattering in the ion chamber would not cause electrons to miss the target. The target chamber was surrounded by paraffin moderator contained in a wooden box 32 in. square and 19 in. in the beam direction. Neutrons produced in the target were detected by a pair of enriched  $\text{BF}_3$  proportional counters, each of which extended the length of the box, and which were symmetrically located on opposite sides of the target chamber. Background due to neutrons produced outside the target region was reduced by surrounding the box with a thin layer of boron carbide and an outside layer of paraffin 8 in. thick.

The pulses from each of the proportional counters were amplified, and the large pulses due to the  $(n, \alpha)$  reaction in  $\text{B}^{10}$  were selected by integral discrimination. The scaling circuits were gated off for a period of 7.5  $\mu\text{sec}$  during and following the electron beam pulse. This off-time was found necessary to allow the counters and their associated circuits to recover from the large pile-up of pulses produced when the 0.6- $\mu\text{sec}$  beam pulse struck the target. Since the lifetime of the thermal neutrons in paraffin is approximately 175  $\mu\text{sec}$ , the initial off-time of 7.5  $\mu\text{sec}$  represents a counting loss of  $\sim 3\%$ . When thick targets of high- $Z$  materials were used, it was necessary to limit the intensity of the beam so that the dead-time due to the pile-up of prompt pulses did not exceed 7.5  $\mu\text{sec}$ . To do this the number of recorded neutrons per unit of monitor response was measured as a function of the beam intensity. The limiting value of this ratio as the intensity was lowered was taken as the correct value.

To determine the efficiency of moderating and detecting the neutrons, a RaBe source<sup>12</sup> with a strength of  $(1.00 \pm 0.05) \times 10^5$  neutrons/sec was placed at the position of the target. The combined efficiency of the two  $\text{BF}_3$  counters was found to be  $(0.92 \pm 0.05)\%$ .

<sup>11</sup> W. C. Barber, Phys. Rev. **97**, 1071 (1955).

<sup>12</sup> Manufactured and certified by the Canadian Radium and Uranium Corporation, New York, New York.

<sup>9</sup> K. L. Brown and R. Wilson, Phys. Rev. **93**, 443 (1954).

<sup>10</sup> W. C. Barber, Phys. Rev. **111**, 1642 (1958).

When the gates were used with a pulsed source, the efficiency became 0.89%.

The RaBe source produces an energy spectrum of neutrons different from that produced in photonuclear reactions. Therefore it was considered desirable to test the efficiency calibration with a reaction which produced a known spectrum of neutrons. The most desirable reaction for this purpose was the photodisintegration of the deuteron. This reaction has been extensively investigated in the energy range from threshold to 20 Mev, and the theory checked by experiment is reliable enough to give the absolute cross section correct to 10% anywhere in this energy range.

The neutrons ejected from the deuterons in a heavy-water target have a very anisotropic angular distribution. It was therefore necessary to know the efficiency of the detection system as a function of the angle of emission of the neutron from the target. A first-order approximation was made by describing the counting system as a right-circular cylinder of length  $l$  and radius  $r$  with the property that neutrons emitted in any direction that intersected the walls of the cylinder were counted with fixed efficiency whereas those neutrons directed out the ends of the cylinder escaped without detection. The lengths  $l$  and  $r$  were determined to give the best fit to the curve of counting rate vs axial position observed when the RaBe source was moved along the axis of the target chamber. This simple two-parameter description of the counting system represented the data taken at ten points between the center and one end of the target chamber with an average error of less than 1%. Using this concept of an effective cylinder, the detection efficiency for a source with an angular distribution  $f(\theta)$  relative to that for an isotropic source is given by

$$R = \left[ \int_{\tan^{-1}(r/l)}^{90^\circ} f(\theta) \sin\theta d\theta \right] / \left[ \int_0^{90^\circ} f(\theta) \sin\theta d\theta \right] \times \left[ \int_{\tan^{-1}(r/l)}^{90^\circ} \sin\theta d\theta \right] / \left[ \int_0^{90^\circ} \sin\theta d\theta \right]^{-1}. \quad (1)$$

The best-fit value of  $r/l$  was 0.80.

The yield of neutrons from a target thickness of 0.698 g/cm<sup>2</sup> of heavy water in a thin-walled polystyrene holder was measured as a function of electron energy both with and without a 0.437-g/cm<sup>2</sup> aluminum radiator ahead of the target. To evaluate the background due to neutrons produced in the oxygen of the target, the carbon of the holder, and extraneous sources, similar measurements were made with a holder containing ordinary distilled water. The net observed yields as a function of primary electron energy were converted to total yields using Eq. (1) together with the angular distributions observed by Halpern and Weinstock.<sup>13</sup> The results are shown in Fig. 2. For comparison, the

<sup>13</sup> J. Halpern and E. V. Weinstock, Phys. Rev. **91**, 934 (1953).

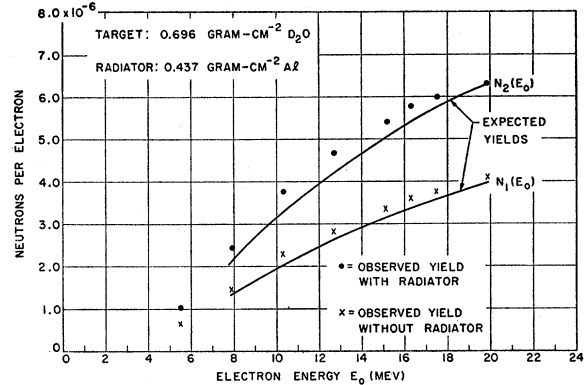


FIG. 2. Comparison of measured neutron yields from deuterium with expected yield curves calculated from the photodisintegration cross section.

expected yields from these targets were computed from the cross sections for the electric- and magnetic-dipole disintegration given by Feshbach and Schwinger.<sup>14</sup> (The contribution of electric-quadrupole disintegration to the cross section is negligible in this energy range.) The expected yields were computed taking into account the energy loss by ionization and radiation of the primary beam as it traversed the target materials. The direct disintegration of the deuteron by the electron beam was computed from the photodisintegration cross section by the virtual photon spectrum method first developed by Weizsäcker and Williams<sup>15</sup> and later extended by others.<sup>16</sup> The yield due to real photons was computed using the "integrated-over-angles" Bethe-Heitler bremsstrahlung formula. In the case where no aluminum radiator was in front of the target, slightly over half of the yield was due to the direct effect of the electrons. The expected yields are shown as solid curves in Fig. 2. There has been no normalization in either the curves or the points of the figures. The experimental yields are higher than the computed ones by an average amount of 7.5%, which is certainly within the combined error of the RaBe source calibration and the uncertainty in the deuteron cross section. There is a systematic decrease in the discrepancy between theory and experiment as the electron energy is increased. This could be due to a variety of causes including errors in the deuteron cross section, systematic errors in the thick-target corrections, or neutron energy dependence of the detector efficiency. The good over-all agreement the calibrations with the RaBe neutrons and the deuterium neutrons, which have widely differing energy spectra, indicates that the energy dependence of the detector efficiency is not an important source of error in the photoneutron yield measurements. All

<sup>14</sup> H. Feshbach and J. Schwinger, Phys. Rev. **84**, 194 (1951).

<sup>15</sup> C. F. V. Weizsäcker, Z. Physik **88**, 612 (1934); E. J. Williams, Kgl. Danske Videnskab. Selskab, Mat.-fys. Medd. **13**, 4 (1935).

<sup>16</sup> R. H. Dalitz and D. R. Yennie, Phys. Rev. **105**, 1598 (1956), discuss the limitations of the method and give references to previous work.

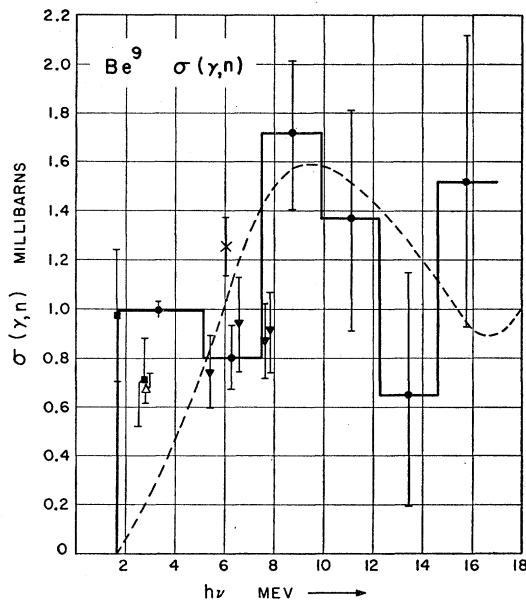


FIG. 3. Cross section for the  $\text{Be}^9(\gamma, n)$  reaction as determined from a number of experiments: circles, present measurements; dashed curve, Nathans and Halpern (reference 18); cross, Carver, Kondaiah, and McDaniel [Phil. Mag. 45, 948 (1954)]; squares, Russel, Sacks, Wattenberg, and Fields [Phys. Rev. 73, 545 (1948)]; triangle, Snell, Barber, and Sternberg [Phys. Rev. 80, 637 (1950)]; inverted triangles, V. O. Eriksen and C. P. Zaleski [J. phys. radium 15, 492 (1954)].

elements above about  $Z=30$  should have similar neutron spectra. The measurements of Cortini *et al.*<sup>6</sup> on neutrons from chromium and tantalum support this conclusion.

### RESULTS

The calibration of the neutron detector efficiency makes it possible to establish an absolute scale for the

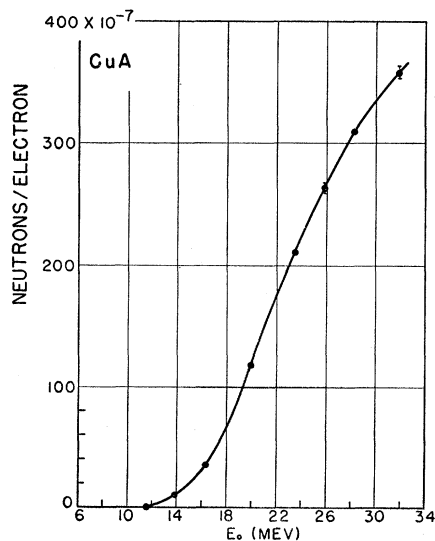


FIG. 4. Neutron yield curve as a function of initial electron energy for a natural Cu target 0.108-radiation-length thick.

relative  $\text{Be}^9(\gamma, n)$  cross section as a function of photon energy reported by Barber.<sup>10</sup> These measurements were made with targets of Be (with and without an aluminum radiator) in the same geometry as was used for the heavy-water experiment. The result for the  $\text{Be}^9(\gamma, n)$  cross section up to 17 Mev is shown as a histogram in Fig. 3. In obtaining this curve the observed counter efficiency for the isotropic RaBe neutron source was corrected using Eq. (1) with  $f(\theta)=1.2\pm\sin^2\theta$ , which is the angular distribution of neutrons observed by Fabricand *et al.*<sup>17</sup> The vertical lines on the histogram indicate expected standard errors for the cross section averaged over each energy interval. These errors are large because the cross section was derived from a yield curve and differences were involved. The error in the

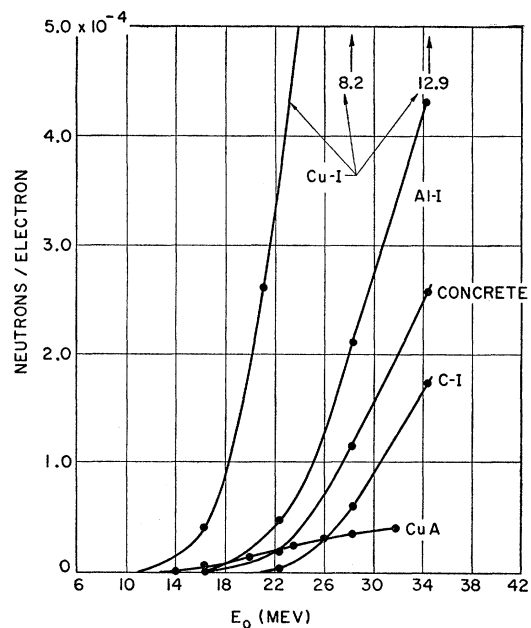


FIG. 5. Yield of neutrons per incident electron as a function of initial electron energy for the low- $Z$  elements. The concrete target is a simple 3:1 sand:cement mixture. The numbers at the top right refer to the Cu-I curve at the indicated energies.

determination of the integrated cross section is almost independent of the errors caused by taking differences, and the uncertainties in the absolute calibration of the neutron detectors and in the angular distribution of the neutrons are the main sources of error. These considerations lead to an estimated standard error of  $\pm 15\%$  on the integrated cross section of 18 Mev-mb derived from Fig. 3.

Figure 4 shows the total neutron yield from a natural copper target of 0.108-radiation-length thickness. Errors on the data points are statistical.

Figures 5-11 present the data for thick targets; Table I gives the thicknesses of all targets. The yields presented in Figs. 5-11 were computed under the

<sup>17</sup> Fabricand, Allison, and Halpern, Phys. Rev. 103, 1755 (1956).

assumption that the neutrons are emitted isotropically. This is likely to be nearly true for the heavy elements. In carbon, a distribution  $1+1.5 \sin^2\theta$  is expected from the shell-model picture of the giant resonance. Our computed yields would be 7.5% too high in this case.

### DISCUSSION

#### $\text{Be}^9(\gamma, n)$

The  $\text{Be}^9(\gamma, n)$  cross section as determined in a number of experiments is shown in Fig. 3. Except for the first region from 1.7 to 3 Mev, our results are in agreement with those of Nathans and Halpern,<sup>18</sup> which were also obtained by the photon-difference method. The meas-

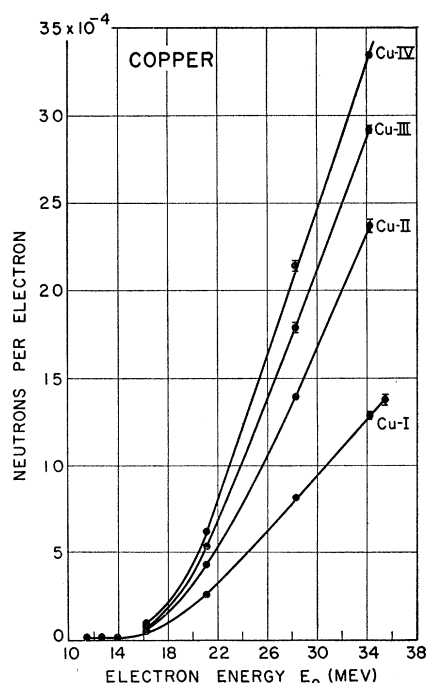


FIG. 6. Yield of neutrons per incident electron as a function of initial electron energy for natural Cu targets of various thicknesses. The Roman numerals give the target thicknesses to the nearest integral number of radiation lengths.

urements made with monoenergetic  $\gamma$ -rays in the low-energy region indicate that in the region from 1.7 to 3 Mev our cross section is probably too high whereas that of Nathans and Halpern is too low. In this energy region the thick-target corrections to the bremsstrahlung spectrum are difficult to evaluate, and for this reason we believe the points measured with monoenergetic  $\gamma$ -rays are more accurate than those determined using a bremsstrahlung spectrum. The value of the cross section integrated to 17 Mev ( $18 \pm 3$  Mev-mb) agrees with that obtained by Nathans and Halpern<sup>18</sup> (16.5 Mev-mb).

<sup>18</sup> R. Nathans and J. Halpern, Phys. Rev. **92**, 940 (1953).

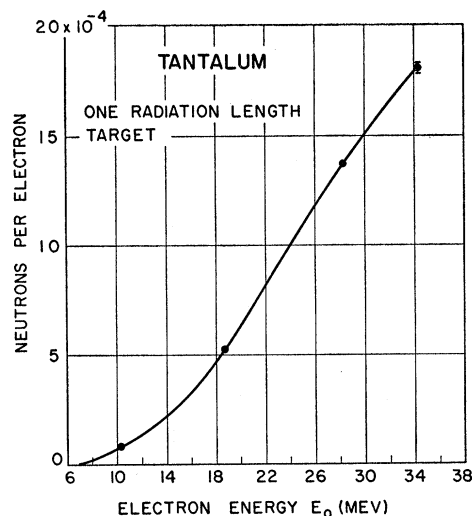


FIG. 7. Yield of neutrons per incident electron as a function of initial electron energy for the Ta target 1 radiation-length thick.

#### $\text{Cu}(\gamma, pn)$

The total neutron yield from Cu, 0.108-radiation-length thick, is shown in Fig. 4. The measurements of Brown and Wilson<sup>9</sup> on the electrodisintegration of  $\text{Cu}^{63}$  were used to subtract the direct electro-induced yield from the total yield, and the results of the total photo-neutron yield are shown as solid circles in Fig. 12. Also shown are the  $(\gamma, n)$  and  $(\gamma, 2n)$  yields from  $\text{Cu}^{63}$  determined by Berman and Brown,<sup>19</sup> normalized so that the curves agree in the region below 20 Mev. Above 20 Mev, the neutron yield in excess of that due to  $(\gamma, n)$  and  $(\gamma, 2n)$  can be attributed to the  $(\gamma, pn)$  reaction. Since we used natural copper and are subtracting normalized data from  $\text{Cu}^{63}$ , we make the assumption

TABLE I. Thicknesses of the targets used in the experiment, with the exception of heavy water, all targets contained isotopes in their naturally-occurring proportions.

Target	Thickness (g/cm <sup>2</sup> )	Thickness (radiation lengths)
Heavy water	0.698	"thin"
Be	0.589	0.00867
C-I	38.91	0.88
Al-I	24.19	1.00
Cu-A	1.372	0.108
Cu-I	13.26	1.04
Cu-II	26.56	2.08
Cu-III	39.86	3.13
Cu-IV	53.13	4.17
Ta-I	6.21	0.98
Pb-I	5.88	1.01
Pb-II	11.42	1.97
Pb-III	17.30	2.98
Pb-IV	22.89	3.94
Pb-VI	34.42	5.93
U-I	6.17	1.14
U-II	12.42	2.30
U-III	18.61	3.46
Concrete	28.5	1.19

<sup>19</sup> A. I. Berman and K. L. Brown, Phys. Rev. **96**, 83 (1954).

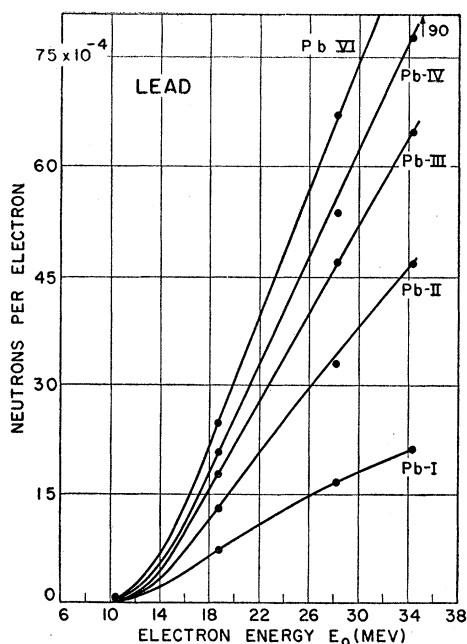


FIG. 8. Yield of neutrons per incident electron as a function of initial electron energy for the natural lead targets of various thicknesses. The number 90 refers to the value of the VI curve at the indicated energy.

that the various cross sections in  $\text{Cu}^{65}$  are proportional to those in  $\text{Cu}^{63}$ . This will not be strictly true, but  $\text{Cu}^{65}$  is only 31% abundant and the errors from the assump-

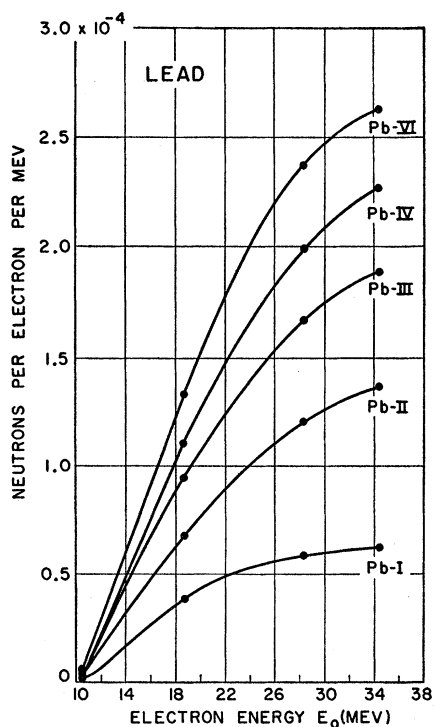


FIG. 9. Yield of neutrons per incident electron per Mev as a function of initial electron energy for Pb targets.

tion will be reduced correspondingly. The photon-difference method of determining the cross section, as described by Katz and Cameron,<sup>20</sup> was applied to the  $(\gamma, pn)$  yield data obtained directly by subtraction of the crosses from the solid curve in Fig. 12. The yield is given by

$$Y(E_0) = N_e N_T N_R \int_{E_{th}}^{E_0} \varphi(E_0, k, t) \sigma(k) dk, \quad (2)$$

where  $k$  is the quantum energy in Mev;  $N_e$  is the number of incident electrons of energy  $E_0$ ;  $N_R$  is the number of nuclei per  $\text{cm}^2$  in the effective radiator producing the bremsstrahlen;  $N_T$  is the number of

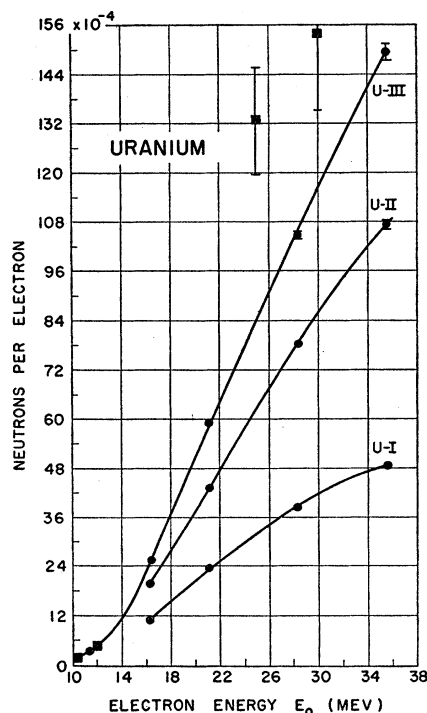


FIG. 10. Yield of neutrons per incident electron as a function of electron energy for natural uranium targets of various thicknesses. The results of the calculation by Biram (reference 1) are shown by solid squares.

nuclei per  $\text{cm}^2$  in the target;  $\varphi(E_0, k, t)$  is the bremsstrahlung cross section in  $\text{cm}^2/\text{Mev}$  interval for the radiator of effective thickness  $t$ ;  $\sigma(k)$  is the  $(\gamma, pn)$  reaction cross section; and  $E_{th}$  is the threshold energy for the reaction.

Figure 13 is the  $(\gamma, pn)$  cross section as obtained by the photon-difference method for determining  $\sigma(k)$  from Eq. (2). The maximum occurs at  $\sim 21$  Mev and the half-width is  $\sim 5$  Mev. The many assumptions used in deriving this curve makes its features uncertain, and details of the shape should not be taken seriously.

A comparison of the present results with the isotopic  $(\gamma, n)$  cross section determined by Berman and Brown<sup>19</sup>

<sup>20</sup> L. Katz and A. G. W. Cameron, Can. J. Phys. 29, 518 (1951).

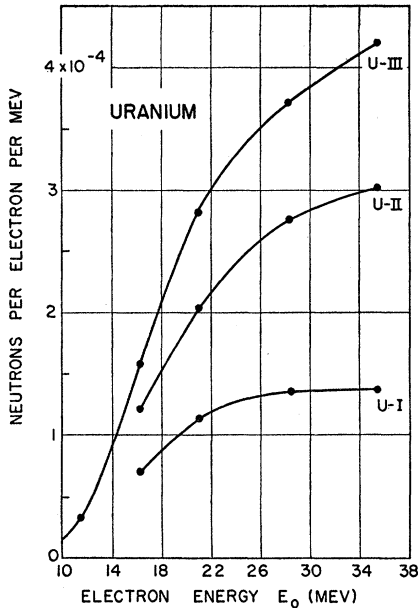


FIG. 11. Yield of neutrons per incident electron per Mev as a function of initial electron energy for the uranium targets.

indicates a ratio of 1.39 for the (natural/Cu<sup>63</sup>) integrated cross sections. Sagane<sup>21</sup> states that the (Cu<sup>65</sup>/Cu<sup>63</sup>) cross-section ratio is 2.0. Using Sagane's result, a ratio of 1.31 is obtained for the (natural copper/Cu<sup>63</sup>) integrated cross sections. This 6% difference is within experimental error.

A value for the ( $\gamma, pn$ ) integrated cross section about four times larger than that of the ( $\gamma, 2n$ ) integrated cross section is indicated by the results. Similar results have been observed previously: for example, Ghoshal<sup>22</sup> found that the compound nucleus of Zn<sup>64</sup>, formed by

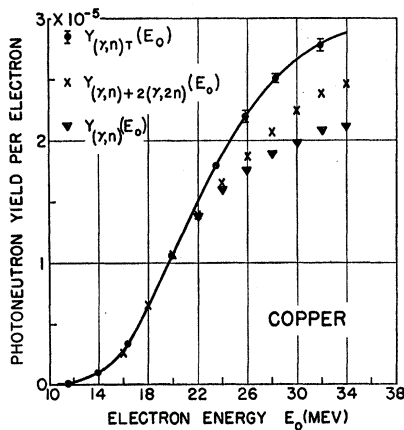


FIG. 12. Yield of neutrons per incident electron as a function of initial electron energy for the Cu target (0.108 radiation length). The yield shown is due to photodisintegration only. Plotted also are the data of Berman and Brown (reference 19) for Cu<sup>63</sup>.

<sup>21</sup> R. Sagane, Phys. Rev. 83, 174 (1951).

<sup>22</sup> S. N. Ghoshal, Phys. Rev. 80, 939 (1950).

either  $\alpha$ -particle bombardment of Ni<sup>60</sup> or proton bombardment of Cu<sup>63</sup>, preferred the ( $pn$ ) decay mode over the ( $2n$ ) decay mode by a factor of 4.

**Thick Targets**

The yield of neutrons per electron of energy  $E_0$  incident on a target containing  $t$  radiation lengths can be expressed as

$$Y(E_0, Z, t) = n(Z) \int_0^{E_0} l(E_0, k, Z, t) \sigma(Z, k) dk, \quad (3)$$

where  $n(Z)$  is the number of atoms/cm<sup>2</sup> in one radiation length of a target of atomic number  $Z$ ;  $l(E_0, k, Z, t)$  is the track length of photons of energy  $k$  in the shower developed in the target; and  $\sigma(Z, k)$  is the cross section for a photon of energy  $k$  to produce a neutron from the target. Levinger<sup>23</sup> applied Eq. (3) to the case of an

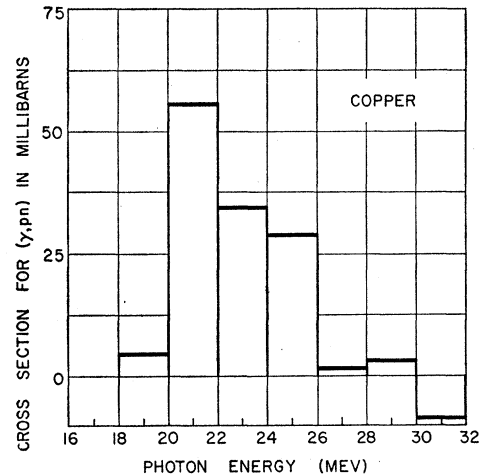


FIG. 13. Cross section for the reaction ( $\gamma, pn$ ) as a function of photon energy for Cu.

infinite lead target to obtain the result

$$Y(E_0, 82, \infty) = 2 \times 10^{-4} E_0 (\text{Mev}) \text{ (neutrons/electron)}. \quad (4)$$

In deriving this result, Levinger used experimental data for  $\sigma$ . For the track length he used the expression

$$l(E_0, k, 82, \infty) = 0.8 (E_0/k^2), \quad (5)$$

which differs by a factor of 1.4 from the high-energy shower theory result. The modification is required because the photons of importance in neutron production have absorption cross sections smaller than the asymptotic limit assumed in the theory. The experimental data for the Pb target of 6 radiation lengths agree with Eq. (4) at  $E_0 = 25$  Mev. However, at higher energy Eq. (4) predicts lower yields and at lower energies higher yields than are observed experimentally.

The measured yields were still increasing with thick-

<sup>23</sup> J. S. Levinger, Nucleonics 6, No. 5, 64 (May, 1950).

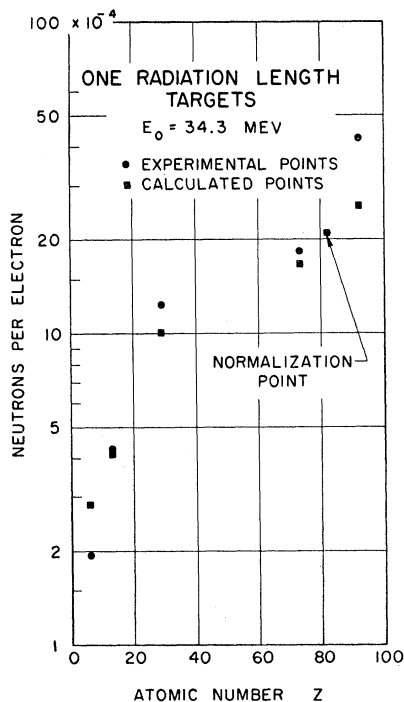


FIG. 14. Experimental and expected yields of neutrons per incident electron for 1-radiation-length targets at 34.3 Mev, as a function of atomic number  $Z$ . The experimental yields were obtained by dividing the measured yields from the targets labeled I by the actual target thicknesses listed in Table I. The expected yields were calculated from expression (8).

ness up to 6 radiation lengths, which was the thickest target used. An estimate of the additional yield expected from an infinite target can be obtained from Wilson's Monte Carlo study of showers.<sup>24</sup> The data presented by Wilson include the ionization produced by incident electrons of various energies from 50 to 500 Mev in lead targets as a function of target thickness. A curve for 34-Mev electrons was obtained by extrapolation of his data. The 34-Mev curve contained 9.2% of the total energy of the shower in the tail beyond 6 radiation lengths. The spectrum of photons in the tail of the shower is known to consist primarily of photons between 2 and 20 Mev where the absorption coefficient in lead is minimum. We expect these photons to be less efficient in producing neutrons than the photon spectrum at the shower maximum; however, the spectrum shape is not known well enough for a reliable calculation. An empirical procedure which should give a fair approximation to the neutron yield from the tail is to compare the energy contained in each thickness interval of the shower with the measured neutron yields from the same interval. This comparison at 34 Mev shows that the ratio of neutron yield to energy loss as a function of depth in the shower is fairly constant out to 4 radiation lengths where it begins to drop. From this we know that the percentage neutron production

<sup>24</sup> R. R. Wilson, Phys. Rev. 86, 261 (1952).

in the tail of the shower beyond 6 radiation lengths is less than the percentage energy production of 9.2%. A neutron yield estimate of  $(5 \pm 3)\%$  from the tail of the shower is the best that can be obtained from this analysis.

Equation (3) can be used as a basis for understanding the  $Z$ -dependence of the measured neutron yields shown in Fig. 14. As a first approximation we take  $l$  proportional to  $E_0/k^2$  as predicted by high-energy shower theory. Also, since this is a function which does not vary rapidly over the giant resonance region, we replace the integral in Eq. (3) by  $(E_0/k_0^2) \int \sigma(Z, k) dk$ , where  $k_0$  is the photon energy at the maximum of the cross section, which from theory is proportional to  $A^{-1/2}$ . If we estimate the integrated cross section from the sum-rule result for the absorption of  $\gamma$ -rays,  $\int \sigma(Z, k) dk \propto (NZ/A)$ , we find that the expression for the yield from a 1-radiation-length target is proportional to

$$\frac{1}{Z^2 \ln(183A^{-1/2})} E_0 A^{1/2} \frac{NZ}{A} = \frac{1}{\ln(183A^{-1/2})} \frac{E_0 N}{A^{1/2} Z}, \quad (6)$$

where  $N = A - Z$ . This expression decreases slowly with increasing  $Z$  whereas the observed yields (Fig. 14) increase rather strongly with  $Z$ .

The disagreement stems from the fact that the photoneutron integrated cross sections are much lower than the sum-rule result in light elements, and from our neglect of electron energy loss by ionization in estimating the track length of photons. The assumption of a  $k^{-2}$  dependence of the track length for the photons is not bad in spite of the facts that the targets are only 1 radiation-length thick and the photon energies involved are of the same magnitude as the critical energy. This is because the thin-target bremsstrahlung spectrum is nearly proportional to  $1/k$  and the thick-target spectrum, generated by compounding thin-target spectra of all electron energies from the incident energy on down, is thus nearly proportional to  $k^{-2}$ .

The yield estimated can be greatly improved by using measured parameters of the neutron production cross sections in place of the sum-rule result and by taking ionization loss into account by writing the track length as

$$l(E_0, k_0, Z) \propto \frac{R(Z)}{I(Z) + R(Z)} \frac{E_0}{k_0^2}, \quad (7)$$

where  $R(Z)$  and  $I(Z)$  are the values of the electron radiation loss and ionization loss;  $R$  and  $I$  are also functions of electron energy, but for computation of the  $Z$ -dependence of the yield it is a fairly good approximation to use an average electron energy effective in producing the photons which in turn produce neutrons. The expected  $Z$ -dependence of the neutron yield per electron for targets of one radiation length is then

proportional to the expression

$$\left( \int \sigma(Z, k) dk \right) \frac{R(Z)}{I(Z) + R(Z)} \frac{E_0}{k_0^2(Z)} \frac{t_r(Z)}{A}, \quad (8)$$

where  $t_r(Z)$  is the number of g/cm<sup>2</sup> in one radiation length;  $A$  is the atomic weight of the target material;  $\int \sigma(Z, k) dk$  is the integrated cross section for producing a neutron by any reaction; and  $k_0(Z)$  is the photon energy at the peak of the cross section.

In Table II values of the quantities in expression (8) are tabulated for the measured target elements using  $E_0 = 34.3$  Mev. The values for  $\int \sigma dk$  are taken from the neutron yield measurements of Montalbetti, Katz, and Goldemberg,<sup>25</sup> and Nathans and Halpern.<sup>26</sup> (For those cases where the same element was measured by both experiments the average result is used.) The values of (8) were arbitrarily normalized to agree with the experimental yield for lead and then plotted as squares on Fig. 14. With the exception of uranium, where additional neutrons are produced by fission, the agreement with the experimental points is good. This agreement indicates that (8) can be used as a fairly reliable guide in obtaining the yield of neutrons per electron from other thick targets.

A detailed calculation of the expected neutron yield from a uranium target was made by Biram.<sup>1</sup> A Monte Carlo method was used to determine the photon spectrum resulting from the bremsstrahlung of the primary electrons (25–40 Mev) in a thick target. All the important photon absorption processes were taken into account, and hence the result should be more accurate than those based on extrapolations of high-energy shower theory. The results of the calculation are shown as solid squares on Fig. 10, where the indicated errors are those given by Biram.<sup>1</sup> At 30 Mev, the calculated yields are 33% greater than our experimental yields from the 3.46-radiation-length target. The calcu-

<sup>25</sup> Montalbetti, Katz, and Goldemberg, Phys. Rev. **91**, 659 (1953).

<sup>26</sup> R. Nathans and J. Halpern, Phys. Rev. **93**, 437 (1954).

TABLE II. Calculation of the  $Z$ -dependence of neutron yields by means of expression 8.

Element	$\int_0^{34.3} \sigma dk$ (Mev-mb)	$k_0$ (Mev)	$t_r$ (g/cm <sup>2</sup> )	$I$ at 30 Mev (Mev-g <sup>-1</sup> -cm <sup>2</sup> )	$R$ at 30 Mev (Mev-g <sup>-1</sup> -cm <sup>2</sup> )	Expected yield (8)	Expected yield (normalized to experimental Pb yield) ×10 <sup>4</sup>
C	50	23	44	1.7	0.44	2.45	2.84
Al	132	19.2	24.4	1.7	0.79	3.53	4.10
Cu	870	18.5	12.4	1.5	1.6	8.72	10.1
Ta	3800	15	6.4	1.25	3.0	14.4	16.6
Pb	4800	13.7	5.8	1.2	3.3	18.0	20.8
U	7200	13.8	5.4	1.2	3.6	22.4	25.9

lation assumed the target thick enough to absorb all primary and secondary quanta. The yield from Pb targets increases by about one third when the target thickness is increased from 3.46 radiation lengths to infinity. A similar increase is to be expected in the case of uranium, which would produce a yield in agreement with the calculation. The Harwell measurements have been reported<sup>2</sup> to support the Biram calculation at the higher primary energies.

A yield curve for a uranium target 0.75 in. thick extending from 10- to 80-Mev primary electron energy was measured by Baldwin *et al.*<sup>3</sup> Their curve indicates a remarkable constancy in the number of neutrons produced per unit of beam energy at all energies above 35 Mev. Below 35 Mev, the shape of their curve differs considerably from any of ours (Fig. 11). However, their target was almost twice as thick as our largest one and the results should not be comparable in all detail.

#### ACKNOWLEDGMENTS

We should like to thank Professor W. K. H. Panofsky for his support and advice concerning this work. We wish to acknowledge the valuable contributions made by D. Lloyd in constructing experimental equipment and by Dr. K. L. Brown in discussion of experimental problems.